

Dynamical instability of differentially rotating stars

Masaru Shibata, Shigeyuki Karino, and Yoshiharu Eriguchi

Department of Earth Science and Astronomy, Graduate School of Arts and Sciences, University of Tokyo, Komaba, Meguro, Tokyo 153-8902, Japan

Accepted ???? Month ??, Received ???? Month ??; in original form 2002 April 1

ABSTRACT

We study the dynamical instability against bar-mode deformation of differentially rotating stars. We performed numerical simulation and linear perturbation analysis adopting polytropic equations of state with the polytropic index $n = 1$. It is found that rotating stars of a high degree of differential rotation are dynamically unstable even for the ratio of the kinetic energy to the gravitational potential energy of $O(0.01)$. Gravitational waves from the final nonaxisymmetric quasistationary states are calculated in the quadrupole formula. For rotating stars of mass $1.4M_{\odot}$ and radius several 10 km, gravitational waves have frequency several 100 Hz and effective amplitude $\sim 5 \times 10^{-22}$ at a distance of ~ 100 Mpc.

Key words: gravitational waves – stars: neutron – stars: rotation – stars: oscillation.

1 INTRODUCTION

Stars in nature are rotating and subject to nonaxisymmetric rotational instabilities. An exact treatment of these instabilities exists only for incompressible equilibrium fluids in Newtonian gravity (Chandrasekhar 1969; Tassoul 1978). For these configurations, global rotational instabilities arise from nonradial toroidal modes $e^{im\varphi}$ ($m = \pm 1, \pm 2, \dots$) when $\beta \equiv T/W$ exceeds a certain critical value. Here φ is the azimuthal coordinate and T and W are the rotational kinetic and gravitational potential energies. In the following we will focus on the $m = \pm 2$ bar-mode since it is expected to be the fastest growing mode (but see Centrella et al. (2001) with regard to a counter-example for extremely soft equations of state).

There exist two different mechanisms and corresponding timescales for bar-mode instabilities. Uniformly rotating, incompressible stars in Newtonian theory are *secularly* unstable to bar-mode deformation when $\beta \geq \beta_s \simeq 0.14$. However, this instability can only grow in the presence of some dissipative mechanism, like viscosity or gravitational radiation, and the growth time is determined by the dissipative timescale, which is usually much longer than the dynamical timescale of the system. By contrast, a *dynamical* instability to bar-mode deformation sets in when $\beta \geq \beta_d \simeq 0.27$. This instability is independent of any dissipative mechanisms, and the growth time is determined typically by the hydrodynamical timescale of the system.

For the compressible case, determining the onset of the dynamical bar-mode instability, as well as the subsequent evolution of an unstable star, requires numerical computations. Hydrodynamical simulations performed in Newtonian theory (Tohline et al. 1985; Durisen et al. 1986; Williams &

Tohline 1987,1988; Tohline & Hachisu 1990; Houser et al. 1994; Smith et al. 1995; Houser & Centrella 1996; Pickett et al. 1996; Toman et al. 1998; Imamura et al. 2000; New et al. 2000; Brown 2000; Liu & Lindblom 2001; Liu 2001) have shown that β_d is ~ 0.27 as long as the rotational profile is not strongly differential. In this case, once a bar has developed, the formation of spiral arms plays an important role in redistributing the angular momentum and forming a core-halo structure. Recently, it has been shown that β_d can be smaller for stars with a higher degree of differential rotation (Centrella et al. 2001; Tohline & Hachisu 1990; Pickett et al. 1996; Liu & Lindblom 2001; Liu 2001) as $\beta_d \sim 0.14$. In such case, the formation of bars and spiral arms does not take place. Instead, small density perturbation is excited and left to be weakly nonlinear. To date, there is no report of dynamically unstable stars with $\beta \lesssim 0.14$.

There are numerous evolutionary paths which may lead to the formation of rapidly and differentially rotating neutron stars. β increases approximately as R^{-1} during stellar collapse. Also, with decreasing stellar radius, the angular velocity in the central region may be much larger than that in the outer region. During supernova collapse, the core contracts from $\sim 1,000$ km to several 10 km, and hence β increases by two orders of magnitude. Thus, even rigidly rotating progenitor stars with a moderate angular velocity may yield rapidly and differentially rotating neutron stars which may reach the onset of dynamical instability (Bonazzola & Marck 1993; Rampp et al. 1998). Similar arguments hold for accretion induced collapse of white dwarfs to neutron stars and for the merger of binary white dwarfs to neutron stars. Differential rotation is eventually suppressed by viscous angular momentum transfer or magnetic braking (Baumgarte

arXiv:gr-qc/0206002v2 6 Jun 2002

2000), but within the transport timescale, the differentially rotating stars are subject to nonaxisymmetric instabilities.

In this Letter, we report some of results we have recently obtained on dynamical bar-mode instabilities in differentially rotating stars. We pay attention to rotating stars with a high degree of differential rotation in Newtonian gravity using both linear perturbation analysis and nonlinear hydrodynamical simulation. The detail of our study will be summarized in a future paper (Shibata et al. in preparation). Here, we highlight a new finding.

2 METHOD

To investigate the dynamical stability, we first prepare rotating stars in equilibrium. Rotating stars in equilibrium are modeled by the polytropic equations of state as $P = K\rho^\Gamma$ where P , ρ , K and Γ denote the pressure, density, polytropic constant and adiabatic index. Here, we choose $\Gamma = 2$ to model moderately stiff equations of state for neutron stars. For simplicity, the profile of the angular velocity Ω is set as

$$\Omega = \frac{\Omega_0 A^2}{\varpi^2 + A^2}, \quad (1)$$

where A is a constant, Ω_0 the angular velocity at the symmetric axis, and ϖ cylindrical radius ($\sqrt{x^2 + y^2}$). A controls the steepness of the rotational profile: For smaller A , the profile is steeper and for $A \rightarrow \infty$, the rigid rotation is recovered. In the limit of A going to 0, this rotation law gives uniform specific angular momentum, which is the limiting law allowed by axisymmetric stability analyses. (Here, however, $A = 0$ is prohibited in this situation because angular velocity diverges along the rotation axis.) This is also the rotation law that has been often used in studies of nonaxisymmetric instabilities in tori and annuli (Papaloizou & Pringle 1984; Goodman & Narayan 1988; Andalib et al. 1997). In this Letter, we report the results for $\hat{A} \equiv A/R = 0.3$ and 1 where R is the equatorial radius of rotating stars.

In a linear perturbation analysis, we derive the linear perturbation equations of the hydrodynamic equations and substitute the functions in the form $f(r, \theta)e^{im\varphi - i\omega t}$ for perturbed hydrodynamic variables. As a result, the problem reduces to the eigen value problem for determining a complex value of ω and the corresponding eigen functions of the perturbed quantities. The details of the numerical method will be reported in future (Karino & Eriguchi in preparation).

In the hydrodynamical simulation, we initially superimpose a density perturbation of the bar-mode in the form

$$\delta\rho = \delta \cdot \rho_0 \frac{x^2 - y^2}{R^2}, \quad (2)$$

where ρ_0 denotes the axisymmetric configuration and δ constant. Namely, we focus on a fundamental mode (f-mode) for which there is no node. In this work, we choose $\delta = 0.1$, and the velocity is left to be unperturbed at $t = 0$. The growth of a bar-mode can be followed by monitoring the distortion parameter

$$\eta \equiv \frac{I_{xx} - I_{yy}}{I_{xx} + I_{yy}}, \quad (3)$$

where I_{ij} denotes the quadrupole moment

$$I_{ij} = \int d^3x \rho x^i x^j. \quad (4)$$

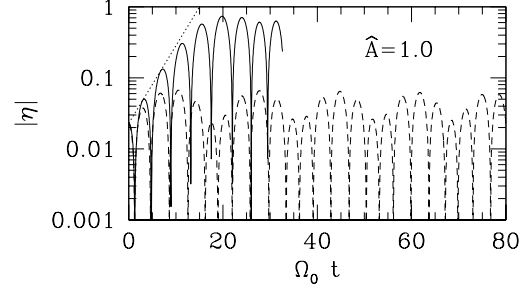


Figure 1. $|\eta|$ as a function of $\Omega_0 t$ for $\hat{A} = 1$ with $C_a = 0.255$ (solid line) and 0.305 (dashed line). The dotted line denotes the growth rate of the unstable mode.

Simulations were performed using a 3D numerical code in Newtonian gravity (Shibata et al. 1997). We adopt a fixed uniform grid with size $141 \times 141 \times 141$ in $x - y - z$, which covers an equatorial radius by 50 grid points initially. To confirm that the results depend weakly on the resolution, we also perform test simulations with size $71 \times 71 \times 71$ (i.e., the grid spacing becomes twice larger) for several selected cases. We assume a reflection symmetry about the equatorial plane. Since many rotating stars we pick up have flattened configuration, we set the grid spacing of z half of that of x and y .

3 NUMERICAL RESULTS

First we show results for rotating stars of moderately large differential rotation with $\hat{A} = 1$. In Fig. 1, we show $|\eta|$ as a function of time for $C_a = R_p/R = 0.255$ and 0.305, where R_p is the polar radius. It is found that for $C_a = 0.255$, the rotating stars are dynamically unstable, while for $C_a = 0.305$, they are stable. In Fig. 2, we also display ω_r/Ω_0 and ω_i/Ω_0 as a function of β . Here, ω_r was derived by carrying out the Fourier transformation of $\eta(t)$, and ω_i was measured using the growth rate of the peaks of $|\eta|$ (see dotted line in Fig. 1). We also compute these angular frequencies by a linear perturbation analysis (solid lines). We find that two results independently obtained agree fairly well. The linear analysis also indicates that this unstable mode is likely to be the f-mode (of no node in the eigen function).

We find that at $C_a \sim 0.3$, the dynamical stability changes. In terms of β , the stability changes at $\beta \sim 0.26$ for $\hat{A} = 1$. Thus, β_d is not extremely smaller than that for rigidly rotating incompressible stars (Chandrasekhar 1969) in the case when the degree of the differential rotation is not very high.

The situation drastically changes for $\hat{A} = 0.3$. In Fig. 3, we show $|\eta|$ as a function of time for $C_a = 0.405$, 0.605, and 0.805 obtained by numerical simulations. Note that for $C_a = 0.805$, $\beta \approx 0.04$. We find that in every model, non-axisymmetric dynamical instabilities take place. In Fig. 4, we also show ω_r/Ω_0 and ω_i/Ω_0 as a function of β . Since several growing modes seem to be excited simultaneously for $C_a = 0.605$ and 0.805, we plot upper and lower bounds for ω_i . Results by numerical simulations agree again with those by linear perturbation analysis. The linear analysis

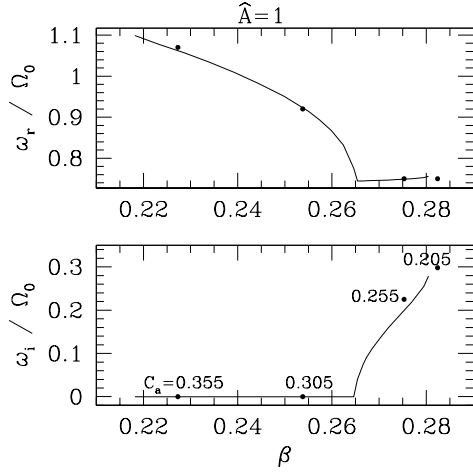


Figure 2. ω_r/Ω_0 and ω_i/Ω_0 as a function of β for $\hat{A} = 1$. The solid curves and solid circles denote the results by linear perturbation analysis and numerical simulation, respectively. We choose results for $C_a = 0.205, 0.255, 0.305$ and 0.355 .

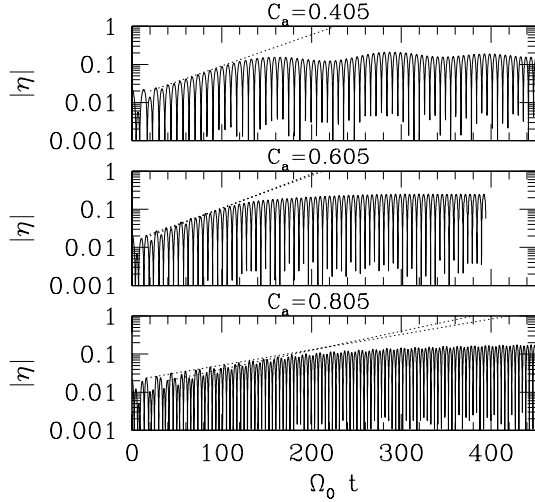


Figure 3. $|\eta|$ as a function of $\Omega_0 t$ for $\hat{A} = 0.3$ with $C_a = 0.405$ (upper) 0.605 (middle), and 0.805 (lower). The dotted lines denote the growth rate of the unstable modes. For $C_a = 0.605$ and 0.805 , we plot two dotted lines which indicate the upper and lower bounds of the growth rates.

also indicates that even for $\beta \approx 0.03$, the rotating stars are dynamically unstable.

In Fig. 5, we display the contour line and velocity vectors for $C_a = 0.605$ at selected time slices as an example. We find that the dynamical instability does not excite large spiral arms and fragmentations. Rather, it saturates in a weakly nonlinear stage at which $|\eta| \sim 0.2$, to form a quasistationary ellipsoid. We note that this feature is independent of C_a as long as $\hat{A} = 0.3$.

Since the rotating stars of $C_a \lesssim 0.85$ change to non-axisymmetric objects, they can be sources of gravitational waves. In Fig. 6, we show the gravitational waveforms along the z -axis ($h_{+,x}$) and energy luminosity (\dot{E}) as a function of time for $C_a = 0.605$. We note that the results for other models are qualitatively the same as that in Fig. 6. Here,

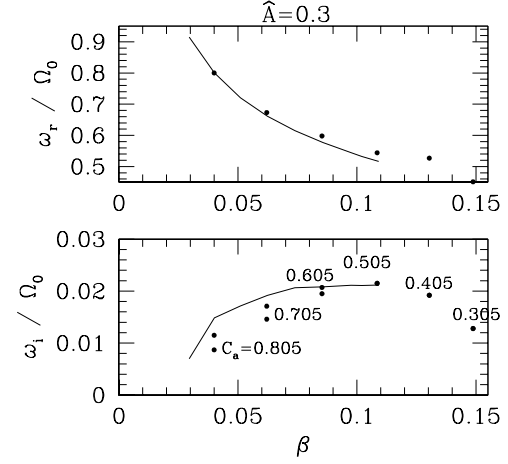


Figure 4. The same as Fig. 2, but for $\hat{A} = 0.3$. For $C_a \geq 0.605$, upper and lower bounds of ω_i for results in numerical simulations are shown.

gravitational waves are calculated in the quadrupole formula (Misner et al. 1973), and we define

$$h_+ \equiv \frac{\ddot{I}_{xx} - \ddot{I}_{yy}}{r}, \quad h_{\times} \equiv \frac{2\ddot{I}_{xy}}{r}, \quad \text{and} \quad \dot{E} \equiv \frac{1}{5} \mathcal{F}_{ij}^{(3)} \mathcal{F}_{ij}^{(3)} \quad (5)$$

where $\ddot{I}_{ij} = d^2 I_{ij}/dt^2$, $\mathcal{F}_{ij} = I_{ij} - \delta_{ij} I_{kk}/3$, $\mathcal{F}_{ij}^{(3)} = d^3 \mathcal{F}_{ij}/dt^3$, and r is the distance from a source to a detector. Here, we use the units $c = G = 1$. Since the outcome of the dynamical instability is a quasistationary ellipsoid, the amplitude and luminosity of gravitational waves settle down to a nearly constant value as $rh_{+,x} \sim 0.2(M^2/R)$ and $\dot{E} \sim 0.01(M/R)^5$.

4 DISCUSSIONS

Using the results shown in Fig. 6, we can estimate the expected amplitude of gravitational waves from the non-axisymmetric outcome formed after the dynamical instability saturates. Here, we pay particular attention to protoneutron stars likely formed soon after the supernovae of mass $\sim 1.4M_{\odot}$ and radius several 10 km. For the maximum amplitude of gravitational waves $h \sim 0.2M^2/Rr$, and the energy luminosity $\dot{E} \sim 0.01(M/R)^5$, the emission timescale of gravitational waves can be estimated as

$$\tau \sim \frac{T}{\dot{E}} \sim 100\beta' \left(\frac{R}{M} \right)^4 M, \quad (6)$$

where we set $T = \beta' M^2/R$ and $0.04 \lesssim \beta' \lesssim 0.4$ for $\hat{A} = 0.3$ and $0.3 \leq C_a \leq 0.8$. The characteristic frequency of gravitational waves is denoted as

$$f \equiv \frac{\omega_r}{2\pi} \approx 800\text{Hz} \left(\frac{\xi}{2} \right) \left(\frac{15M}{R} \right)^{3/2} \left(\frac{M}{1.4M_{\odot}} \right)^{-1}, \quad (7)$$

where $\xi \equiv \omega_r \sqrt{R^3/M} \sim 2$ (see Figs. 4 and 7). Since the cycles of gravitational wave-train N are estimated as $N \equiv f\tau$, the effective amplitude of gravitational waves $h_{\text{eff}} = \sqrt{N}h$ is

$$h_{\text{eff}} \approx 5 \times 10^{-22} \left(\frac{\xi}{2} \right)^{1/2} \left(\frac{\beta'}{0.1} \right)^{1/2} \left(\frac{R}{15M} \right)^{1/4}$$

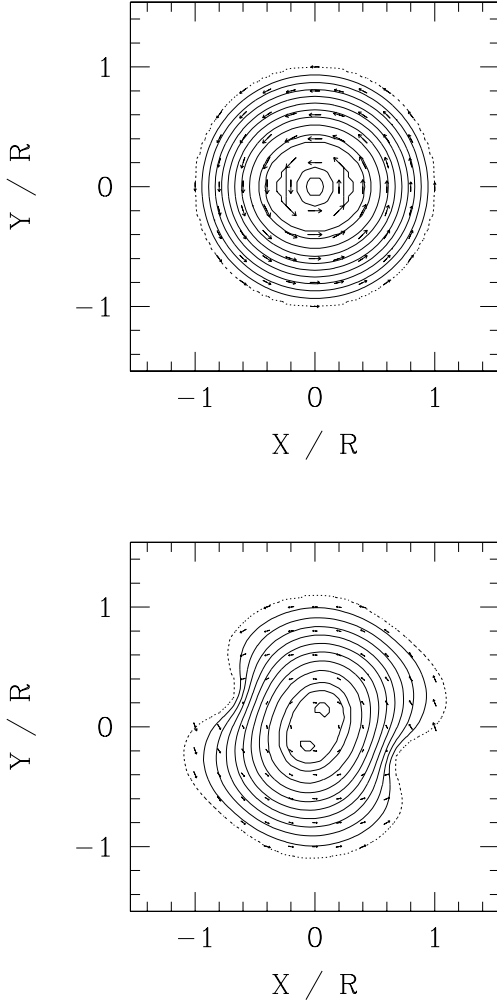


Figure 5. Snapshots of density contour lines and velocity vectors in the equatorial plane at $t = 0$ (left) and $\Omega_0 t \approx 390$ (right) for $\hat{A} = 0.3$ and $C_a = 0.605$. The contour lines are drawn for $\rho/\rho_{\max} = j/10$ ($j = 1 \sim 9$) and 0.95 (solid curves) and for $\rho/\rho_{\max} = 0.01$ (dotted curve), where ρ_{\max} denotes the maximum density.

$$\times \left(\frac{M}{1.4M_{\odot}} \right) \left(\frac{100\text{Mpc}}{r} \right) \quad (8)$$

(Thorne 1987; Lai & Shapiro 1995; Liu & Lindblom 2001; Liu 2001). Thus, gravitational waves from protoneutron stars of a high degree of differential rotation and of mass $\sim 1.4M_{\odot}$ and radius several 10 km in the distance of ~ 100 Mpc can be a source for laser interferometric detectors such as LIGO (Thorne 1995). We emphasize that f and h_{eff} depend weakly on β (or β') for $\hat{A} = 0.3$. This implies that even if the star is not rapidly rotating, the dynamical instability can set in and as a result, differentially rotating stars can emit gravitational waves of a large amplitude.

To summarize, we have studied dynamical bar-mode instability of differentially rotating stars focusing on the f-mode. We have found that rotating stars of a high degree of differential rotation are dynamically unstable against non-axisymmetric deformation even for $\beta \ll 0.27$.

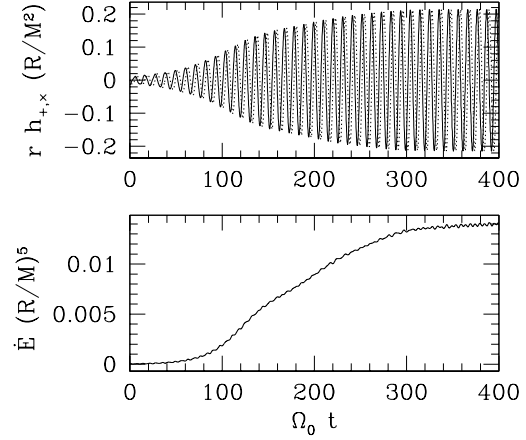


Figure 6. Gravitational waves for $\hat{A} = 0.3$ and $C_a = 0.605$. Upper figure: h_+ (solid curve) and h_{\times} (dotted curve) in units of M^2/R as a function of $\Omega_0 t$. Lower figure: \dot{E} in units of $(M/R)^5$.

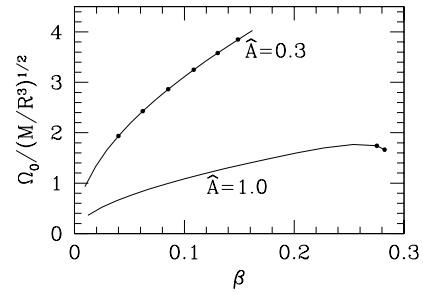


Figure 7. $\Omega_0/\sqrt{M/R^3}$ as a function of β . The solid circles denote the dynamically unstable stars we found.

It is worthy to note that the real parts of the eigen frequencies do not vanish but approach to finite values as the value of β decreases, i.e. in the spherical limit. This behavior is totally different from those of the r-modes (see e.g. Karino et al. 2001), several self-gravity induced instability modes of slender tori or annuli such as I-modes and J-modes (Goodman & Narayan 1988; Andalib et al. 1997), or shear instability modes (or P-modes) such as Papaloizou-Pringle instability for toroids (Papaloizou & Pringle 1984) and for spheroids (Luyten 1990). Therefore, we have identified the unstable modes we find in this paper as the f-mode.

The physical mechanism for the onset of dynamical instabilities found in this Letter may be explained in the following manner: For a small value of \hat{A} , non-spherical deformation of a stellar configuration is significant around the rotational axis although the distant part from the rotational axis is almost spherical. Thus, with decrease of the value of C_a , most rotational energies are confined to the region near the rotational axis. Increase of the rotational energy can be much larger than those of the gravitational and internal energies, because the overall shape cannot be much different from that of a sphere. As a result, the total energy becomes large with small values of C_a . However, if the rotational energy exceeds a certain amount in the region near the rotational axis, there may exist other equilibrium configurations with lower total energies, as in the case of bifurcation of

the Jacobi ellipsoidal sequence from the Maclaurin sequence (Chandrasekhar 1969). In fact, the total energy of the Jacobi ellipsoid is lower than the Maclaurin spheroid of the same mass and the angular momentum, if the rotational energy exceeds a certain criterion.

Once the instability sets in, the axisymmetric star begins to change its shape to a nonaxisymmetric configuration. In such case, the angular velocity in the region near the rotational axis, $\sim \Omega_0$, is very large (larger than $\sqrt{M/R^3}$). It implies that, despite of the large rotational energy, the angular momentum cannot be very large because $T \sim \int (x^2 + y^2) \times \Omega_0^2 dm$ and $J \sim \int (x^2 + y^2) \times \Omega_0 dm$, where J and dm are the angular momentum and the mass element, respectively. Therefore, even if the nonaxisymmetric mode grows due to the dynamical instability, the configuration cannot be highly elongated or form spiral-arm structures; i.e., there exists a saturation state of a small nonaxisymmetric deformation. For the bar-mode instability of the Maclaurin spheroids, the rotational energy is "confined" to the outer part of the configuration by making the shape very flat and so the angular momentum can be also large, even though the angular velocity is not extremely large ($< \sqrt{M/R^3}$). Therefore, once a bar-mode dynamical instability sets in, configurations can be considerably different from the original spheroidal shapes.

It is possible that other non-fundamental modes have larger ω_i than the f-mode has. However, the present study shows that there exists at least one mode which induces the nonaxisymmetric deformation. Such rotating stars subsequently form nonaxisymmetric structures and hence can be a source of laser interferometric gravitational wave detectors.

ACKNOWLEDGMENTS

We thank Lee Lindblom for discussion and comments. We are grateful to Luciano Rezzolla for his careful reading and comments. Numerical simulations were performed on FACOM VPP5000 in the data processing centre of National Astronomical Observatory of Japan. This work was in part supported by a Japanese Monbu-Kagakusho Grant (No. 12640255 and 13740143). SK is supported by JSPS Research Fellowship for Young Scientists.

REFERENCES

- Andalib, S. W., Tohline, J. E. & Christodoulou, D. M. 1997, *ApJ Suppl.*, 108, 471
 See, e.g., Baumgarte, T. W., Shapiro, S. L. & Shibata, M., 2000, *ApJL*, 528, L29
 Bonazzola, S. & Marck, J.-A., 1993, *A & A*, 267, 623
 Brown, J. D., 2000, *Phys. Rev. D*, 62, 084024
 Centrella, J. M., New, K. C. B., Lowe, L. & Brown, J. D., 2001, *ApJL*, 550, 193
 Chandrasekhar, S., 1969, *Ellipsoidal Figures of Equilibrium* (New Haven: Yale University Press).
 Durisen, R. H., Gingold, R. A., Tohline, J. E. & Boss, A. P., 1986, *ApJ*, 305, 281
 Goodman, J. & Narayan, R. 1988, *MNRAS*, 231, 97
 Houser, J. L. & Centrella, J. M., 1996, *Phys. Rev. D*, 54, 7278
 Houser, J. L., Centrella, J. M. & Smith, S. C., 1994, *Phys. Rev. Lett.*, 72, 1314

- Imamura, J. N., Durisen, R. H. & Pickett, B. K., 2000, *ApJ*, 528, 946
 Karino, S. & Eriguchi, Y., in preparation.
 Karino, S., Yoshida, S. & Eriguchi, Y., 2001, *Phys. Rev. D* 64, 024003
 Lai, D. & Shapiro, S. L., 1995, *ApJ*, 442, 259
 Liu, Y. T. & Lindblom, L., 2001, *MNRAS*, 342, 1063
 Liu, Y. T., preprint (gr-qc/0109078)
 Luyten, P. J., 1990, *MNRAS*, 245, 614
 Misner, C. W., Thorne, K. S. & Wheeler, J. A., 1973, *Gravitation* (New York: W. H. Freeman & Company)
 New, K. C. B., Centrella, J. M. & Tohline, J. E., 2000, *Phys. Rev. D*, 62, 064019
 Papaloizou, J.C.B. & Pringle, J.E. 1984, *MNRAS*, 208, 721
 Pickett, B. K., Durisen, R. H. & Davis, G. A., 1996, *ApJ*, 458, 714
 Rampp, M., Müller, E., & Ruffert, M., 1998, *A & A*, 332, 969
 Shibata, M., Karino, S. & Eriguchi, Y., in preparation.
 Shibata, M., Oohara, K. & Nakamura, T., 1997, *Prog. Theor. Phys.*, 98, 1081
 Smith, S., Houser, J. L. & Centrella, J. M., 1995, *ApJ*, 458, 236
 Tassoul, J., 1978, *Theory of Rotating Stars* (Princeton: Princeton University Press)
 Thorne, K. S., 1987, 300 Years of Gravitation, edited by Hawking, S & Israel, W., (Cambridge: Cambridge University Press), 330
 See, e.g., Thorne, K. S., 1995, *Proceeding of Snowmass 95 Summer Study on Particle and Nuclear Astrophysics and Cosmology*, eds. Kolb E. W. & Peccei, R., (Singapore: World Scientific), p. 398
 Tohline, J. E., Durisen, R. H. & McCollough, M., 1985, *ApJ*, 298, 220
 Tohline, J. E. & Hachisu, I., 1990, *ApJ*, 361, 394
 Toman, J., Imamura, J. N., Pickett, B. K. & Durisen, R. H., 1998, *ApJ*, 497, 370
 Williams, H. A. & Tohline, J. E., 1987, *ApJ*, 315, 594 ; 1988, *ibid*, 334, 449